PLANT SIGNALING & BEHAVIOR
2016, VOL. 11, NO. 11, e1244594 (5 pages)
http://dx.doi.org/10.1080/15592324.2016.1244594

Taylor & Francis
Taylor & Francis Group

SHORT COMMUNICATION

Increased callose deposition in plants lacking *DYNAMIN-RELATED PROTEIN 2B* is dependent upon *POWDERY MILDEW RESISTANT 4*

Michelle E. Leslie, Sean W. Rogers*, and Antje Heese

Division of Biochemistry, Interdisciplinary Plant Group, University of Missouri-Columbia, Columbia, MO, USA

ABSTRACT

Callose deposition within the cell wall is a well-documented plant immune response to pathogenic organisms as well as to pathogen-/microbe- associated molecular patterns (P/MAMPs). However, the molecular mechanisms that modulate pathogen-induced callose deposition are less understood. We reported previously that *Arabidopsis* plants lacking the vesicle trafficking component DYNAMIN-RELATED PROTEIN 2B (DRP2B) display increased callose deposition in response to the PAMP flg22. Here, we show that increased number of flg22-induced callose deposits in *drp2b* leaves is fully dependent on the callose synthase POWDERY MILDEW RESISTANT 4 (PMR4). We propose that in addition to functioning in flg22-induced endocytosis of the plant receptor, FLAGELLIN SENSING 2, DRP2B may regulate the trafficking of proteins involved in callose synthesis, such as PMR4, and/or callose degradation.

Abbreviations: CalS12, CALLOSE SYNTHASE 12; CAPS, Cleaved amplified polymorphic sequence; DRP2B, DYNAMIN-RELATED PROTEIN 2B; FLS2, FLAGELLIN SENSING 2; GSL5, GLUCAN SYNTHASE-LIKE 5; GFP, Green fluorescent protein; MAMP, Microbe-associated molecular pattern; PAMP, Pathogen-associated molecular pattern; PR1, PATHOGENESIS-RELATED 1; PM, Plasma membrane; Pto, Pseudomonas syringae pv. tomato; PMR4, POWDERY MILDEW RESISTANT 4; ROS, Reactive oxygen species; RbohD, RESPIRATORY BURST HOMOLOG D; TWS, Trainable Weka Segmentation; WT, Wildtype

ARTICLE HISTORY
Received 6 September 2016
Accepted 30 September 2016

KEYWORDS
Arabidopsis thaliana; callose; DYNAMIN-RELATED PROTEIN 2B (DRP2B); Fiji image analysis; flg22; POWDERY MILDEW RESISTANT 4 (PMR4); Trainable Weka Segmentation plug-in

Plants perceive extracellular pathogens and pathogen-/microbe-associated molecular patterns (P/MAMPs) through the activation of receptors at the plant cell surface.[1,2] The PAMP flg22, derived from bacterial flagellin, is recognized by the plant receptor FLAGELLIN SENSING 2 (FLS2).[3,4] Upon flg22 perception by FLS2, a network of immune responses contributing toward pathogen growth restriction, including production of apoplastic reactive oxygen species (ROS), activation of Ca^{2+}-dependent and MAPK signaling cascades, increased salicylic acid and ethylene production, and transcriptional changes are initiated within the host plant.[5-7] Flg22 recognition likewise promotes cell wall modification, specifically the deposition of callose, a β-1,3-glucan polysaccharide, at discrete cell wall sites;[8,9] but its role in immunity against bacterial infection remains unclear. In addition to the described immune responses, flg22 triggers internalization of activated FLS2 from the plasma membrane (PM) and subsequent endosomal trafficking of FLS2 for degradation.[10,11] At later timepoints after flg22 treatment (>2 hours), flg22-sensitivity is restored through new FLS2 synthesis, likely in preparation for subsequent rounds of flg22-signaling and potential infection.[11] The flg22-signaling response network is complex, and current research aims to understand better the crosstalk between and integration of various flg22-responses at the molecular and cellular levels for sustained pathogen resistance.

Our studies recently identified the *Arabidopsis* vesicle trafficking component DYNAMIN-RELATED PROTEIN 2B (DRP2B) as a novel regulator of flg22-signaling responses and immunity against the flagellated bacteria *Pseudomonas syringae* pv *tomato* (*Pto*) DC3000.[12] DRP2B is a large GTPase with the same domain structure as classical mammalian Dynamins that act as molecular scissors to cleave vesicles from a membrane.[13] Interestingly, we found that loss of *DRP2B* differentially affects distinct branches of the flg22-signaling network such that a subset of responses (Ca^{2+} flux, ROS production, callose deposition) are significantly increased in *drp2b* mutant plants, while some responses are unaffected (MAPK activation) and yet others are reduced (PATHOGENESIS-RELATED 1/PR1-pathway).[12] Decreased *PR1* mRNA levels in response to flg22 and bacterial infection correlated with increased susceptibility to pathogenic and nonpathogenic *Pto* DC3000 strains.[12] In agreement with a role for DRP2B in clathrin-mediated endocytosis from the PM,[14,15] we and others found that *Arabidopsis* DRP2B[12] and *Nicotiana benthamiana* DRP2[16] orthologs, respectively, are required for robust flg22-induced endocytosis of FLS2. In *drp2b* loss-of-function mutant plants, a delay in removal of activated FLS2 from the PM correlates with enhanced flg22-induced ROS production and Ca^{2+} flux.[12] However, based on the non-canonical combination of phenotypic defects in *drp2b* plants, it is likely that DRP2B is required for the proper trafficking and regulation of not only FLS2, but

CONTACT Antje Heese heesea@missouri.edu 117 Schweitzer Hall, Columbia, MO 65211.
*Current affiliation: University of Texas-Southwestern Medical Center, Dallas, TX, USA.

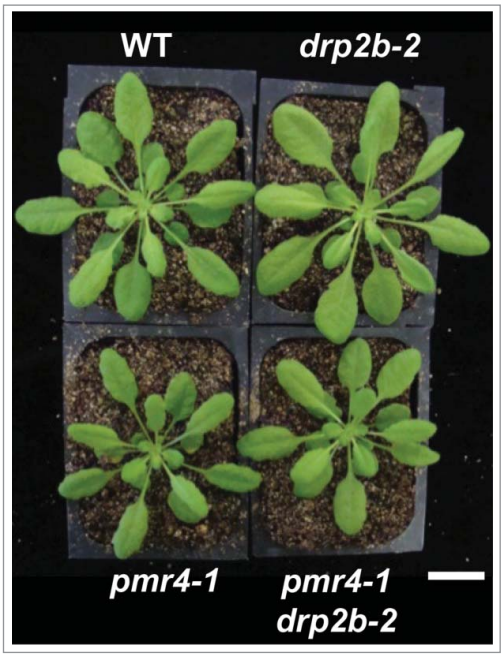

Figure 1. Generation of *pmr4 drp2b* double mutant plants. Five-week old *pmr4-1* and *pmr4-1 drp2b-2* plants grown under short-day (8 hour light/16 hour dark) conditions were smaller than Col-0 wildtype (WT) and *drp2b-2* single mutant plants. Scale bar, 1 cm.

yet unknown cargo proteins that may function in different flg22-signaling branches. Here, we investigate further the genetic requirements for flg22-induced callose production in *drp2b* mutant plants to identify potential cargo proteins to be tested in future studies using targeted approaches.

In both wildtype (WT) and *drp2b* mutant plants, the increase in flg22-induced ROS and callose production requires the NADPH oxidase RESPIRATORY BURST HOMOLOG D (RbohD).[9,12] POWDERY-MILDEW RESISTANT 4 (PMR4)/GLUCAN SYNTHASE-LIKE 5 (GSL5)/CALLOSE SYNTHASE 12 (CalS12) (subsequently referred to as PMR4) is known to be the primary callose synthase required for flg22-induced callose in wildtype plants.[8,17] However, it remains unknown whether PMR4 is responsible for the flg22-induced increase in callose in *drp2b*. To investigate PMR4 contribution to this *drp2b* phenotype, we crossed the *pmr4-1* loss-of-function mutant[18] with *drp2b-2* to generate *pmr4-1 drp2b-2* homozygous double mutant plants (Fig. 1). PCR genotyping for *drp2b-2* (SALK_134887) is described in refs. 12 and 19. To identify the point mutation in *pmr4-1*, we established genotyping by cleaved amplified polymorphic sequence (CAPS) analysis[20] of PCR amplified fragments using primers and restriction enzymes in Table 1. As previously reported for independent loss-of-function *pmr4* alleles (*gls5-2* and *gsl5-3*),[21] *pmr4-1* plants display reduced rosette growth compared to WT plants (Fig. 1). Loss of *DRP2B* did not rescue this growth defect, as *pmr4-1 drp2b-2* plants were consistently smaller and similar in size to *pmr4-1* single mutant plants (Fig. 1).

Next, we infiltrated 3 fully expanded leaves per plant with either a 100 nM flg22 (QRLSTGSRINSAKDDAAGLQIA; Genscript) solution or a mock solution (0.1% DMSO in water). Leaf discs (0.2 cm^2) were collected 24 hours after infiltration, processed and stained with aniline blue as done previously.[12,22] UV-fluorescent, aniline-blue stained callose was imaged with a Leica M205 FA stereoscope (Leica Microsystems, Inc.). For robust quantification of callose deposition, we employed an automated image analysis workflow that we established previously for quantification of fluorescently-labeled, punctate endosomal compartments.[12,23] This method[23] uses freely available Fiji (Fiji is just ImageJ; NIH) software[24] and the Trainable Weka Segmentation (TWS) plug-in[25] for Fiji/ImageJ. After an initial training of the TWS plug-in with 2 or more example images, a model was applied to the entire image dataset resulting in automated segmentation of images such that only fluorescent, punctate callose deposits were detected (Fig. 2, black), while all other fluorescent features (e.g. trichomes, leaf vein architecture) were assigned to background (Fig. 2, white). For each image, the Fiji *Freehand Selection* tool was used to crop and measure the leaf disc area prior to image segmentation. Using the Fiji *Analyze Particles* function, callose deposits were automatically detected and quantified in segmented images within the size range of 50–5,000 μm^2 and circularity index of 0.25–1.00. Detected callose deposits were overlaid upon the original image (Fig. 2, yellow) for visualization of Fiji-TWS results.

In agreement with our previous study,[12] *drp2b-2* leaves exhibited increased flg22-induced callose in comparison to the WT Col-0 (Fig. 3A). Using Fiji-TWS methods, significantly more callose deposits (number per mm^2 of leaf surface) were detected in flg22-infiltrated *drp2b-2* compared to WT ($P < 0.001$) (Fig. 3B). Importantly, the Fiji-TWS image analysis workflow allowed us to expand our analyses, providing evidence that in *drp2b-2* leaves, the significant increase in the number of flg22-induced callose deposits per mm^2 of leaf surface (Fig. 3B) contributed to the previously reported increase in % leaf surface with callose.[12] In control experiments, *pmr4-1* leaves displayed significantly decreased flg22-induced callose production in comparison to WT and *drp2b-2* plants (Fig. 3A–B, $P < 0.0001$). When infiltrated with 100 nM flg22, callose deposition was greatly reduced in *pmr4-1 drp2b-2* leaves to a similar level observed for *pmr4-1* leaves (Fig. 3A). Importantly, no significant differences in the number of callose deposits were observed between the *pmr4-1* single mutant and *pmr4-1 drp2b-2* double mutant (Fig. 3B, $P > 0.05$) indicating

Table 1. *PMR4* genotyping. Plants with *pmr4-1* loss-of-function allele were identified by PCR amplification of genomic DNA with primers spanning the point mutation, followed by CAPS analysis of the PCR product with the indicated restriction enzyme. The expected DNA fragment sizes after restriction analysis of *PMR4* wildtype or *pmr4-1* mutant allele are indicated.

Mutant allele	Primer name	Primer sequence (5′→3′)	CAPS restriction enzyme	CAPS analysis results
pmr4-1 W687Stop (gDNA nt2220 G>A)	*pmr4-1* F *pmr4-1* R	CCAACAAGTTTGCGTTGATCTGG GTGCCACAGCCATTTATCAGGTGCGTC	NheI	*PMR4*: 215 bp *pmr4-1*: 126, 89 bp

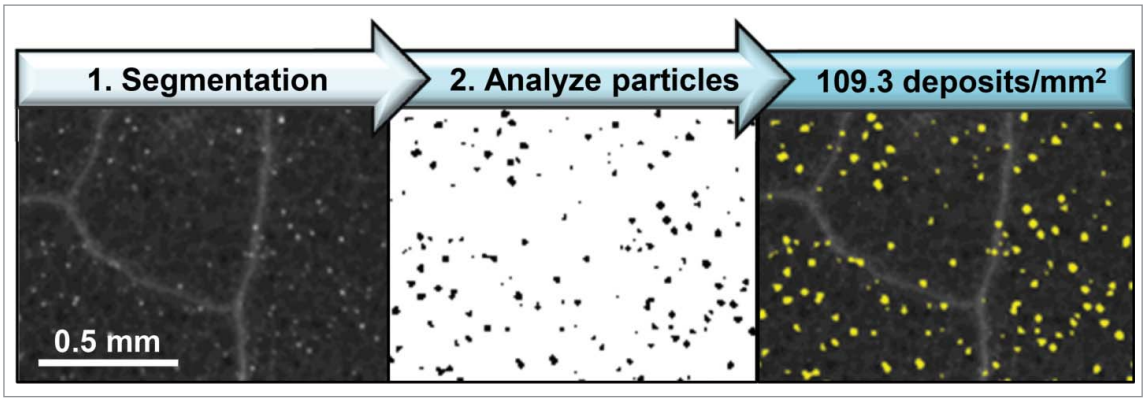

Figure 2. Recognition of flg22-induced callose deposition using Fiji-Trainable Weka Segmentation. Wildtype Col-0 *Arabidopsis* leaf samples were collected 24 hours after infiltration with 100 nM flg22, fixed and stained with aniline blue to visualize sites of callose deposition. The abaxial leaf surface was imaged by UV fluorescence. Images were segmented using established Fiji-TWS methods, and callose deposits were detected (yellow) within the size range of 50–5,000 μm^2 and circularity index of 0.25–1.00.

that the increase in flg22-induced callose deposition is fully dependent on PMR4. Mock-infiltrated leaves served as a control for wound-induced callose deposition, for which no significant differences were observed between Col-0 and *drp2b-2, pmr4-1* or *pmr4-1 drp2b-2* (Fig. 3A–B, $P > 0.5$). Similar results were obtained with an independent mutant allele *pmr4-6*[18] and *pmr4-6 drp2b-2* homozygous double mutant plants (data not shown). Based on comparing flg22-induced callose deposits in WT, single and double mutant plants, we conclude that loss of *DRP2B* results in up-regulation of flg22-induced callose deposition in a PMR4-dependent manner.

These results provide new insight into DRP2B-dependent regulation of late plant immune responses, specifically flg22-induced callose production. In addition to its function in defense-related callose production, PMR4/GSL5 and the closely related GSL1 are jointly required for pollen development.[21] Given that ectopic callose deposition is observed in aborted *drp2a drp2b* double mutant pollen,[19] proteins of the DRP2 family may function more broadly in regulating callose deposition, potentially by regulating multiple GSL/CalS-proteins in plant development and defense. As for PMR4, it has been previously shown that green fluorescent protein (GFP)-tagged PMR4 constitutively expressed in *Arabidopsis* is recruited to sites of attempted penetration of a virulent powdery mildew strain.[26] Whether PMR4 undergoes similar dynamic changes in localization in response to a bacterial pathogen or PAMP (such as flg22) remains to be determined. However, our results suggest the possibility that DRP2B-dependent trafficking events may regulate the localization and/or activity of PMR4 during flg22-induced immune responses. Here, we detected an increased number of callose deposits in *drp2b* plants after flg22 treatment, a phenotype that is fully dependent upon PMR4 (Fig. 3). Additional sites of callose deposition in *drp2b* could result from additional active PMR4 complexes present at the PM, potentially a result of decreased removal of activated PMR4 and/or other regulatory component(s) necessary for robust flg22-induced callose deposition, such as the NADPH oxidase RbohD.[9,12] Such a role for DRP2B in trafficking of defense-related proteins is consistent with our previous findings that DRP2B is required for robust flg22-induced endocytosis of FLS2-GFP from the PM, for which delayed FLS2 internalization correlates with enhanced early Ca^{2+} flux and ROS production in *drp2b*.[12] Alternatively, DRP2B may be required for the expression and/or trafficking of an enzyme(s) required for the

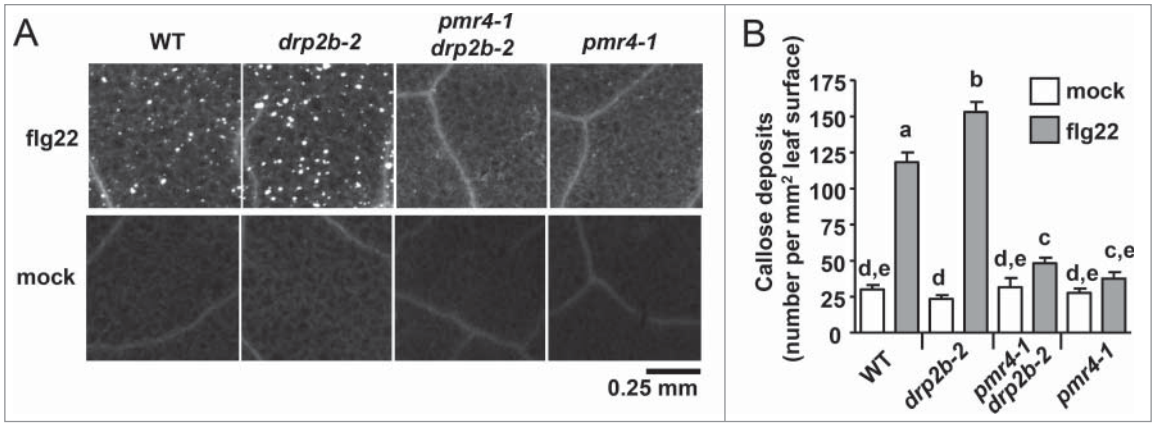

Figure 3. Increased callose deposition in *drp2b* plants is dependent upon the callose synthase PMR4. (A) Representative UV epifluorescent images of aniline blue-stained callose are shown for each genotype and treatment. (B) Quantification of the number of callose deposits per mm^2 of leaf surface using Fiji-TWS methods to automatically detect and analyze callose. For each genotype, n = 33–49 images from 4 flg22-infiltrated plants, and n = 12–24 images from 2 to 3 mock-infiltrated plants. This experiment was repeated twice with similar results. Values are mean ± standard error. Different letters indicate significant differences ($P < 0.05$) while the same letter indicates no significant differences between samples ($P > 0.05$) based on Two-tailed student's t-test.

degradation of callose such as flg22-induced *Arabidopsis* PATHOGENESIS-RELATED 2 protein, a secreted β-1,3-glucanase with known callose-degrading activity.[27]

While callose deposition typically correlates with bacterial immunity,[8] the role of defense-induced callose in bacterial infection remains elusive. In fact, *drp2b* mutants display enhanced flg22-induced callose yet decreased resistance to *Pto* DC3000 infection;[12] thus, further studies are required to understand better the biological role(s) of callose during bacterial infection.

Furthermore, this study extends the use of Fiji-TWS image analysis methods,[23] which we previously established for the study of endosomal FLS2 trafficking,[12] to the analysis of callose deposition. The quantification of aniline-blue stained callose, which fluoresces under UV light, poses challenges since other leaf structures (e.g., trichomes, leaf vein architecture) exhibit high autofluorescence. Using Fiji-TWS methods, dimly fluorescent and low levels of flg22-induced callose deposition (Fig. 3) can be reproducibly quantified. Thus, Fiji-TWS methods[23] provided a sensitive, robust and freely available tool to measure callose deposition that expands the accessibility of quantitative image analysis methods to more researchers than currently available, commercial software applications.[28,29] In the future, more detailed microscopic analyses of callose deposits after various treatments and/or in different genetic backgrounds may further elucidate the role(s) of callose deposition in immune responses to bacteria.

Disclosure of potential conflicts of interest

No potential conflicts of interest were disclosed.

Acknowledgments

We would like to thank ABRC for providing the *pmr4-1* allele, Dr. Shauna Somerville (UC-Berkeley) for providing the *pmr4*-6 allele, the University of Missouri Molecular Cytology Core for microscopy assistance, and all Heese lab members for insightful comments.

Funding

This work was supported by the National Science Foundation-Integrative Organismal Systems under Grant NSF-IOS 1147032 to AH, a University of Missouri - College of Agriculture, Food and Natural Resources Undergraduate Research Internship-Dudley and Virgie Alexander Scholarship to SWR, and a University of Missouri-Monsanto Undergraduate Research Fellowship to SWR.

ORCID

Michelle E. Leslie http://orcid.org/0000-0003-1576-8816
Sean W. Rogers http://orcid.org/0000-0003-1173-6526
Antje Heese http://orcid.org/0000-0003-2711-6153

References

1. Trdá L, Boutrot F, Claverie J, Brulé D, Dorey S, Poinssot B. Perception of pathogenic or beneficial bacteria and their evasion of host immunity: pattern recognition receptors in the frontline. Front Plant Sci 2015; 6:219; PMID: 25904927; http://dx.doi.org/10.3389/fpls.2015.00219
2. Macho AP, Zipfel C. Plant PRRs and the activation of innate immune signaling. Mol Cell 2014; 54:263-72; PMID:24766890; http://dx.doi.org/10.1016/j.molcel.2014.03.028
3. Sun Y, Li L, Macho AP, Han Z, Hu Z, Zipfel C, Zhou J-M, Chai J. Structural basis for flg22-induced activation of the Arabidopsis FLS2-BAK1 immune complex. Science 2013; 342:624-8; PMID:24114786; http://dx.doi.org/10.1126/science.1243825
4. Robatzek S, Wirthmueller L. Mapping FLS2 function to structure: LRRs, kinase and its working bits. Protoplasma 2013; 250:671-81; PMID:23053766; http://dx.doi.org/10.1007/s00709-012-0459-6
5. Nicaise V, Roux M, Zipfel C. Recent advances in PAMP-triggered immunity against bacteria: pattern recognition receptors watch over and raise the alarm. Plant Physiol 2009; 150:1638-47; PMID:19561123; http://dx.doi.org/10.1104/pp.109.139709
6. Boller T, Felix G. A renaissance of elicitors: perception of microbe-associated molecular patterns and danger signals by pattern-recognition receptors. Annu Rev Plant Biol 2009; 60:379-406; PMID:19400727; http://dx.doi.org/10.1146/annurev.arplant.57.032905.105346
7. Tena G, Boudsocq M, Sheen J. Protein kinase signaling networks in plant innate immunity. Curr Opin Plant Biol 2011; 14:519-29; PMID:21704551; http://dx.doi.org/10.1016/j.pbi.2011.05.006
8. Ellinger D, Voigt CA. Callose biosynthesis in Arabidopsis with a focus on pathogen response: what we have learned within the last decade. Ann Bot 2014; 114:1349-58; PMID:24984713; http://dx.doi.org/10.1093/aob/mcu120
9. Luna E, Pastor V, Robert J, Flors V, Mauch-Mani B, Ton J. Callose deposition: A multifaceted plant defense response. Mol Plant Microbe Interact 2011; 24:183-93; PMID:20955078; http://dx.doi.org/10.1094/MPMI-07-10-0149
10. Ben Khaled S, Postma J, Robatzek S. A moving view: subcellular trafficking processes in pattern recognition receptor-triggered plant immunity. Annu Rev Phytopathol 2015; 53:379-402; PMID:26243727; http://dx.doi.org/10.1146/annurev-phyto-080614-120347
11. Smith JM, Salamango DJ, Leslie ME, Collins CA, Heese A. Sensitivity to flg22 is modulated by ligand-induced degradation and de novo synthesis of the endogenous flagellin-receptor FLAGELLIN-SENSING2. Plant Physiol 2014; 164:440-54; PMID:24220680; http://dx.doi.org/10.1104/pp.113.229179
12. Smith JM, Leslie ME, Robinson SJ, Korasick DA, Zhang T, Backues SK, Cornish PV, Koo AJ, Bednarek SY, Heese A. Loss of Arabidopsis thaliana Dynamin-Related Protein 2B reveals separation of innate immune signaling pathways. PLoS Pathog 2014; 10:e1004578; PMID:25521759; http://dx.doi.org/10.1371/journal.ppat.1004578
13. Bednarek SY, Backues SK. Plant Dynamin-Related Protein families DRP1 and DRP2 in plant development. Biochem Soc Transact 2010; 38:797-806; PMID: 20491667; http://dx.doi.org/10.1042/BST0380797
14. Huang J, Fujimoto M, Fujiwara M, Fukao Y, Arimura S, Tsutsumi N. Arabidopsis dynamin-related proteins, DRP2A and DRP2B, function coordinately in post-Golgi trafficking. Biochem Biophys Res Commun 2015; 456:238-44; PMID:25462567; http://dx.doi.org/10.1016/j.bbrc.2014.11.065
15. Fujimoto M, Arimura S, Ueda T, Takanashi H, Hayashi Y, Nakano A, Tsutsumi N. Arabidopsis dynamin-related proteins DRP2B and DRP1A participate together in clathrin-coated vesicle formation during endocytosis. Proc Natl Acad Sci U S A 2010; 107:6094-9; PMID:20231465; http://dx.doi.org/10.1073/pnas.0913562107
16. Chaparro-Garcia A, Schwizer S, Sklenar J, Yoshida K, Petre B, Bos JI, Schornack S, Jones AM, Bozkurt TO, Kamoun S. Phytophthora infestans RXLR-WY effector AVR3a associates with Dynamin-Related Protein 2 required for endocytosis of the plant pattern recognition receptor FLS2. PLoS One 2015; 10:e0137071; PMID:26348328; http://dx.doi.org/10.1371/journal.pone.0137071
17. Chen XY, Kim JY. Callose synthesis in higher plants. Plant Signal Behav 2009; 4:489-92; PMID:19816126; http://dx.doi.org/10.4161/psb.4.6.8359
18. Nishimura MT, Stein M, Hou B-H, Vogel JP, Edwards H, Somerville SC. Loss of a callose synthase results in salicylic acid-dependent disease resistance. Science 2003; 301:969-72; PMID:12920300; http://dx.doi.org/10.1126/science.1086716

19. Backues SK, Korasick DA, Heese A, Bednarek SY. The Arabidopsis Dynamin-Related Protein2 family is essential for gametophyte development. Plant Cell 2010; 22:3218-31; PMID:20959563; http://dx.doi.org/10.1105/tpc.110.077727
20. Neff MM, Turk E, Kalishman M. Web-based primer design for single nucleotide polymorphism analysis. Trends Genet 2002; 18:613-5; PMID:12446140; http://dx.doi.org/10.1016/S0168-9525(02)02820-2
21. Enns LC, Kanaoka MM, Torii KU, Comai L, Okada K, Cleland RE. Two callose synthases, GSL1 and GSL5, play an essential and redundant role in plant and pollen development and in fertility. Plant Mol Biol 2005; 58:333-49; PMID:16021399; http://dx.doi.org/10.1007/s11103-005-4526-7
22. Korasick DA, McMichael C, Walker KA, Anderson JC, Bednarek SY, Heese A. Novel functions of Stomatal Cytokinesis-Defective 1 (SCD1) in innate immune responses against bacteria. J Biol Chem 2010; 285:23342-50; PMID:20472560; http://dx.doi.org/10.1074/jbc.M109.090787
23. Leslie ME, Heese A. Quantitative analysis of ligand-induced endocytosis of FLAGELLIN-SENSING 2 using automated image segmentation. In: Shan L, editor. Methods in Molecular Biology: Plant Pattern Recognition Receptors. Humana Press (in press).
24. Schindelin J, Arganda-Carreras I, Frise E, Kaynig V, Longair M, Pietzsch T, Preibisch S, Rueden C, Saalfeld S, Schmid B, et al. Fiji: an open-source platform for biological-image analysis. Nat Meth 2012; 9:676-82; PMID: 22743772; http://dx.doi.org/10.1038/nmeth.2019
25. Arganda-Carreras I, Kaynig V, Rueden C, Schindelin J, Cardona A, Seung HS. Trainable_segmentation: Release v3.1.2. [Data set]. Zenodo 2016; https://doi.org/10.5281/zenodo.59290
26. Ellinger D, Naumann M, Falter C, Zwikowics C, Jamrow T, Manisseri C, Somerville SC, Voigt CA. Elevated early callose deposition results in complete penetration resistance to powdery mildew in Arabidopsis. Plant Physiol 2013; 161:1433-44; PMID:23335625; http://dx.doi.org/10.1104/pp.112.211011
27. Oide S, Bejai S, Staal J, Guan N, Kaliff M, Dixelius C. A novel role of PR2 in abscisic acid (ABA) mediated, pathogen-induced callose deposition in Arabidopsis thaliana. New Phytol 2013; 200:1187-99; PMID:23952213; http://dx.doi.org/10.1111/nph.12436
28. Hauck P, Thilmony R, He SY. A Pseudomonas syringae type III effector suppresses cell wall-based extracellular defense in susceptible Arabidopsis plants. Proc Natl Acad Sci U S A 2003; 100:8577-82; PMID:12817082; http://dx.doi.org/10.1073/pnas.1431173100
29. Zhou J, Spallek T, Faulkner C, Robatzek S. CalloseMeasurer: a novel software solution to measure callose deposition and recognise spreading callose patterns. Plant Methods 2012; 8:49; PMID:23244621; http://dx.doi.org/10.1186/1746-4811-8-49